AIP | Review of Scientific Instruments

Experimental and simulation study of undesirable short-period deformation in piezoelectric deformable x-ray mirrors

Hiroki Nakamori, Satoshi Matsuyama, Shota Imai, Takashi Kimura, Yasuhisa Sano, Yoshiki Kohmura, Kenji Tamasaku, Makina Yabashi, Tetsuya Ishikawa, and Kazuto Yamauchi

Citation: Review of Scientific Instruments **83**, 053701 (2012); doi: 10.1063/1.4709499
View online: http://dx.doi.org/10.1063/1.4709499
View Table of Contents: http://scitation.aip.org/content/aip/journal/rsi/83/5?ver=pdfcov
Published by the AIP Publishing

Experimental and simulation study of undesirable short-period deformation in piezoelectric deformable x-ray mirrors

Hiroki Nakamori,[1] Satoshi Matsuyama,[1,a)] Shota Imai,[1] Takashi Kimura,[2] Yasuhisa Sano,[1] Yoshiki Kohmura,[3] Kenji Tamasaku,[3] Makina Yabashi,[3] Tetsuya Ishikawa,[3] and Kazuto Yamauchi[1,4]

[1]*Department of Precision Science and Technology, Graduate School of Engineering, Osaka University, 2-1 Yamada-oka, Suita, Osaka 565-0871, Japan*
[2]*Research Institute for Electronic Science, Hokkaido University, Kita 21 Nishi 10, Kita-ku, Sapporo 001-0021, Japan*
[3]*SPring-8/RIKEN, 1-1-1 Kouto, Sayo, Hyogo 679-5198, Japan*
[4]*Center for Ultra-Precision Science and Technology, Graduate School of Engineering, Osaka University, 2-1 Yamada-oka, Suita, Osaka 565-0871, Japan*

(Received 20 February 2012; accepted 16 April 2012; published online 3 May 2012)

To construct adaptive x-ray focusing optics whose optical parameters can be varied while performing wavefront correction, ultraprecise piezoelectric deformable mirrors have been developed. We computationally and experimentally investigated undesirable short-period deformation caused by piezoelectric actuators adhered to the substrate during mirror deformation. Based on the results of finite element method analysis, shape measurements, and the observation of x-ray reflection images, a guideline is developed for designing deformable mirrors that do not have short-period deformation errors. © *2012 American Institute of Physics*. [http://dx.doi.org/10.1063/1.4709499]

I. INTRODUCTION

Recently, x-ray adaptive optics has been advancing rapidly. In a study to realize sub-10 nm focusing in the hard x-ray region, an adaptive mirror placed upstream of a multilayer focusing mirror was used to compensate wavefront errors caused by figure errors on the focusing mirror and deposition errors in the multilayer.[1,2] In addition, adaptive focusing mirrors have been employed in synchrotron radiation facilities to vary optical parameters such as focal length, incident angle, and numerical aperture.[3,4] The former study realized high-quality focusing by controlling the wavefront, whereas the latter study developed an on-site technique for optimizing the optical system for individual experiments.

The present study aims to develop an adaptive focusing system that can vary the optical parameters and control the wavefront by using deformable mirrors. Deformable mirrors that can be flexibly manipulated are essential to realize this.

Previous studies have proposed precise deformable mirrors based on piezoelectric bimorph (or monomorph) actuators.[2,4–7] These mirrors are deformed by expanding and contracting piezoelectric actuators attached to the mirrors by applying voltages to them. It is possible to deform a mirror to a desired shape by controlling the voltages applied to the piezoelectric actuators. Such deformable mirrors can be classified as either separated-piezo mirrors or integrated-piezo mirrors based on their structure. Separated-piezo mirrors consist of a substrate, piezoelectric actuators, and electrodes on the actuators. Using structures with relatively short actuators facilitates the fabrication of large deformable mirrors because it is difficult to manufacture long piezoelectric devices. However, gaps between piezoelectric actuators introduce undesirable deformations with the same dimensions as the gaps;[4] here, we refer to the errors caused by these deformations as high-spatial-frequency (HSF) deformation errors. HSF deformation errors prevent precise wavefront correction. Integrated-piezo mirrors are based on a single piezoelectric actuator with multiple electrodes. They are expected to deform smoothly since they do not have any gaps. However, it is difficult to produce long deformable integrated-piezo mirrors since they require long piezoelectric devices.

There have been no reports of basic guidelines for designing piezoelectric deformable mirrors by comparing deformable mirrors with different structures. In addition, HSF deformation errors have not been investigated in detail.

In this study, both types of deformable mirrors were fabricated. To clearly observe HSF deformation errors, elastic emission machining (EEM) (Ref. 8) was used to remove the inherent waviness of substrates. The deformation errors were investigated in detail by finite element method (FEM) analysis, shape profiling, and observations of x-ray reflection images. In addition, the relationship between distance from the piezoelectric actuator and the amplitude of the deformation errors was examined. The results obtained consistently reveal that separated-piezo mirrors give larger deformation errors than integrated-piezo mirrors. In addition, the line near the piezoelectric actuators is significantly sensitive to the errors and the sensitivity decreased with increasing distance from the piezoelectric actuators. We conclude that the gaps between piezoelectric actuators contribute to the generation of HSF deformation errors and that the errors can be reduced by moving the effective mirror area from the piezoelectric

a)Electronic mail: matsuyama@prec.eng.osaka-u.ac.jp.

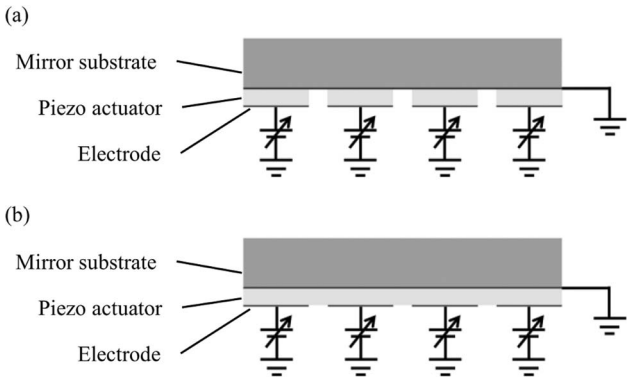

FIG. 1. Schematic of (a) separated-piezo and (b) integrated-piezo mirrors.

actuator. Finally, guidelines were developed for designing piezoelectric deformable mirrors that do not have HSF deformation errors.

II. PIEZOELECTRIC DEFORMABLE MIRRORS

We designed and fabricated both types of deformable mirrors to investigate HSF deformation errors. Both deformable mirrors consist of a substrate and piezoelectric actuators attached to the back of a substrate. A pair of piezoelectric actuators is placed on both sides of the substrate (see Figs. 1 and 2). The effective reflection area is the face at the center of the substrate. Lead zirconate titanate (PZT, piezoelectric constant: -135×10^{-12} m/V, Young modulus: 72 GPa) was employed as the piezoelectric material. Both mirrors have 18 pairs of electrodes, which are used to apply arbitrary voltages to the piezoelectric actuators. Table I lists the specifications of the deformable mirrors. To precisely measure the HSF deformation errors, the intrinsic waviness of the substrates with the same spatial frequency as the deformation errors was removed by EEM and microstitching interferometry (MSI).[9] We focus on shapes with spatial frequencies between 670 and 5000 m^{-1} because a low-spatial-frequency figure can be controlled by the actuators. To determine the

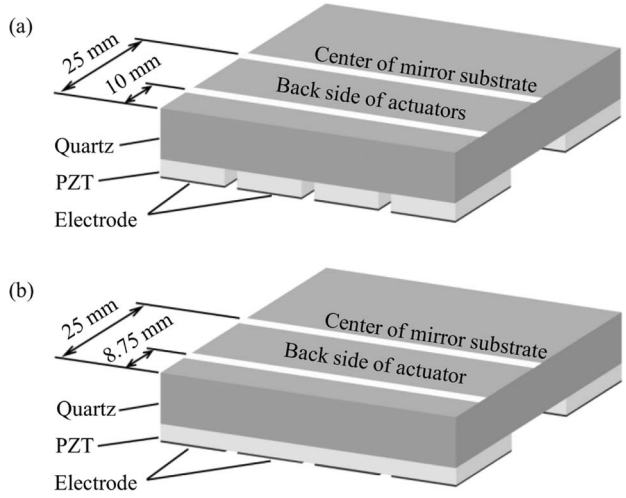

FIG. 2. Processed areas in (a) separated-piezo and (b) integrated-piezo deformable mirrors.

TABLE I. Parameters of deformable mirrors. The two mirrors have different dimensions because they were originally developed for other experiments. The results obtained were carefully compared (see below) by considering the different dimensions.

	Separated	Integrated
Mirror substrate		
Length (mm)	150.0	100.0
Width (mm)	50.0	50.0
Thickness (mm)	5.0	5.0
Coating	Pt (thickness: 100 nm)	
Piezoelectric actuator		
Length (mm)	7.5	100.0
Width (mm)	20.0	17.5
Thickness (mm)	1.0	1.0
Number of parts	18×2	1×2
Electrode length (mm)	7.5	4.8

relationship between the distance from actuators and the deformation error, two lines on the back side of the piezoelectric actuators and the center of the substrate were processed by EEM (see Fig. 2). During the measurement, room temperature was maintained at 25.0 °C, which is the same as the operating temperature of the mirror; this is because a change in temperature will alter the shape of the mirror due to the bimetallic strip effect. Figure 3 shows a figure with a spatial frequency in the range of interest that was extracted from data measured before and after correction. A smoothness of better than 0.5 nm peak-to-valley (PV) was achieved, except for the line on the back side of the piezoelectric actuators of the separated-piezo mirror. This result is discussed later.

III. EXPERIMENTS

A. FEM analysis

Deformation of the mirrors was calculated using commercial FEM software (Pro/Mechanica, Parametric Technology Corporation). To simplify the calculation, the piezoelectric actuators were assumed to expand or contract isotropically. In addition, electric field leakage from the electrodes was ignored. Consequently, only regions of the piezoelectric actuators in contact with the electrodes contribute to mirror deformation. In addition, the adhesive layer between the piezoelectric actuators and the substrate was ignored. FEM simulations that gave the mirror deformation after applying a voltage of 250 V to all the electrodes were performed using the mirror parameters listed in Table I. Shapes with spatial frequencies between 670 and 5000 m^{-1} were then extracted from the obtained shape data.

B. Shape measurements

To investigate HSF deformation errors directly, mirror shapes were measured by MSI before and after applying a voltage of 250 V to all the electrodes. Room temperature was fixed at 25.0 °C to prevent any changes in shape. Shapes with spatial frequencies between 670 and 5000 m^{-1} were then extracted from the obtained shape data.

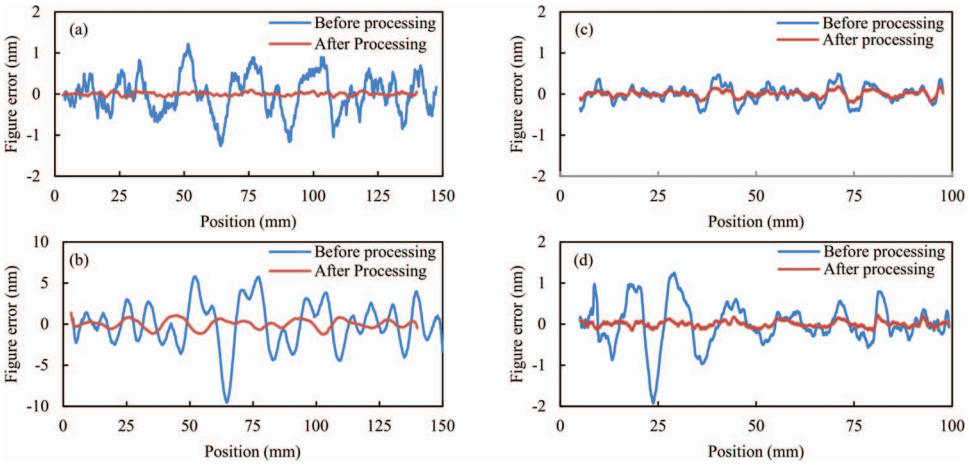

FIG. 3. Figures before and after processing. The short-period shapes were extracted with a spatial frequency filter. (a) and (b) Separated-piezo, and (c) and (d) integrated-piezo mirrors. (a) and (c) At the center of substrate, and (b) and (d) on line on back side of actuators.

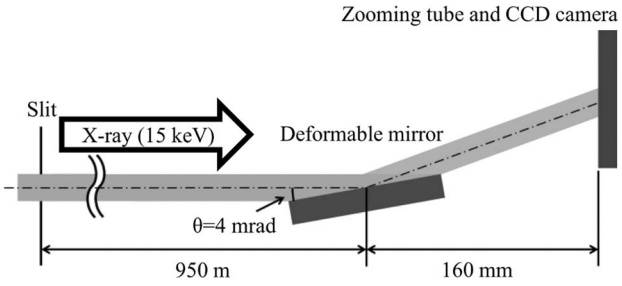

FIG. 4. Schematic of experimental setup to observe x-ray reflection images.

C. Observation of x-ray reflection images

To investigate the effect of HSF deformation errors on x-ray reflections, x-ray images reflected from the deformable mirrors were observed. A reflected image is very sensitive to the surface profile under coherent illumination; speckle patterns are produced from nanoscale protrusions on the reflection surface.[10–12] Figure 4 shows a schematic of the experimental setup at the third experimental hutch of BL29XUL of SPring-8. X-ray images reflected from the mirror before and after applying a voltage of 250 V to all the electrodes were observed using an x-ray zooming tube and a CCD camera (C5333, Hamamatsu Photonics). The temperature of the

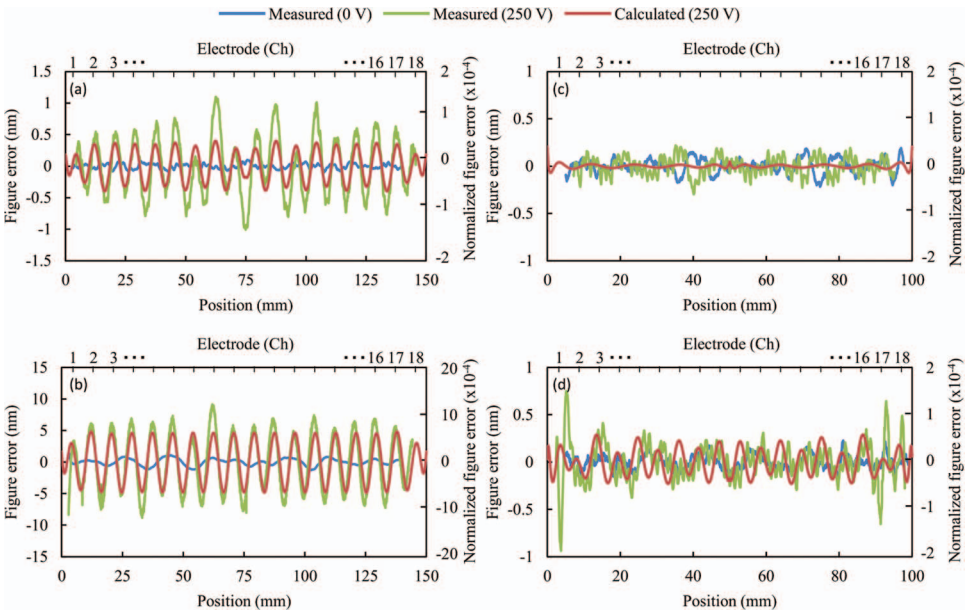

FIG. 5. Measured and calculated HSF deformation errors for (a) and (b) separated-piezo mirror, and (c) and (d) integrated-piezo mirror: (a) and (c) at the center of the substrate, and (b) and (d) on the line on the back side of the actuators. The right vertical axis represents the relative height of the HSF deformation errors normalized by the maximum deformation depth of the substrate. The upper horizontal axis indicates the relative positions of the electrodes.

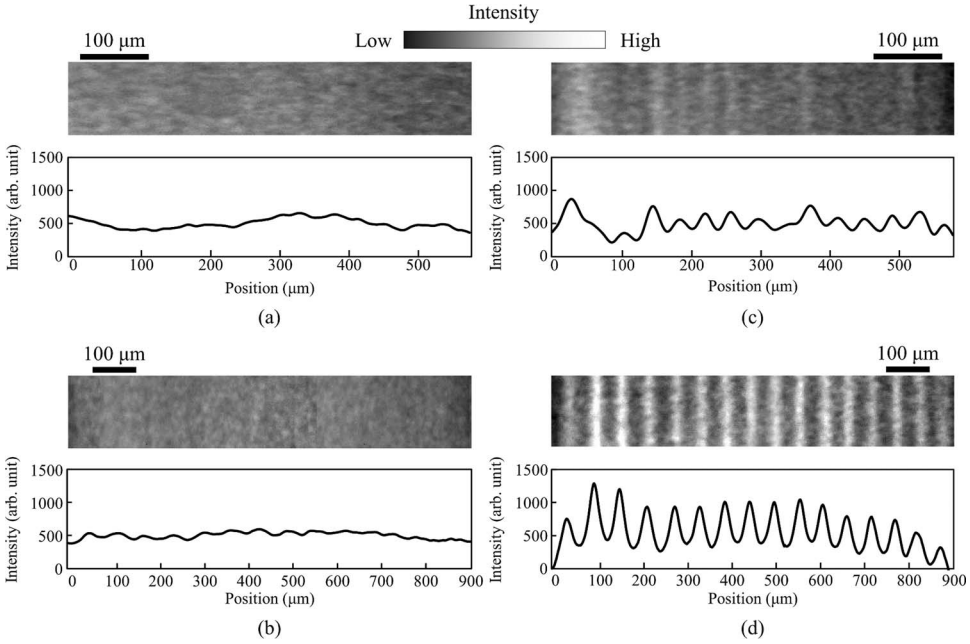

FIG. 6. X-ray reflection images obtained using an separated-piezo mirror (a) and (b) at the center of the substrate, and (c) and (d) on the line on back side of piezoelectric actuator. (a) and (c) Before, and (b) and (d) after applying 250 V.

experimental hutch was controlled to be the same as that in the shape measurements.

IV. RESULTS AND DISCUSSION

Figures 5(a)–5(d) show the measured and calculated shapes, which are in good agreement with each other. This demonstrates that the measurements and simulations were performed well. Application of a voltage of 250 V deformed the integrated-piezo and separated-piezo mirrors into quasi-cylindrical shapes with maximum depths of 4.5 and 7 μm, respectively. For the separated-piezo mirror, HSF deformation errors of 1.5 and 10 nm PV with the same spatial frequency as the piezoelectric actuators were observed on the center line and the line on the back side of the piezoelectric actuators, respectively. For the integrated-piezo mirror, errors of 1 nm PV with the same spatial frequency as the electrodes were observed on the line on the back side of the piezoelectric actuators. In contrast, no HSF deformation errors were observed at the center. Thus, considering the differences in the deformation amplitude, we found that the deformation errors in the separated-piezo mirrors are approximately 10 times

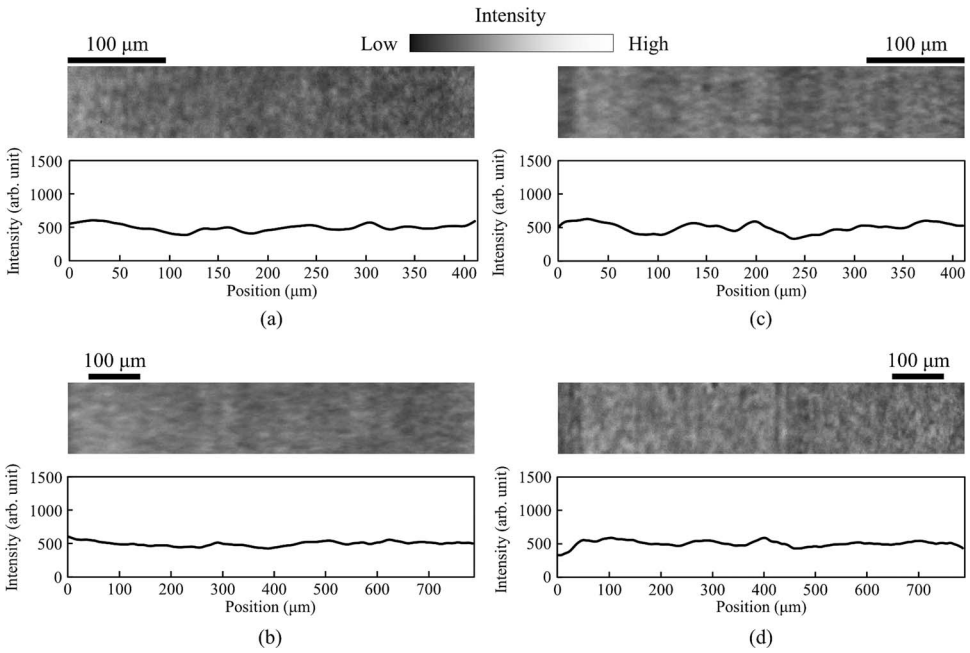

FIG. 7. X-ray reflection images obtained using a integrated-piezo mirror (a) and (b) at the center of the substrate, and (c) and (d) on line on back side of piezoelectric actuator. (a) and (c) Before, and (b) and (d) after applying 250 V.

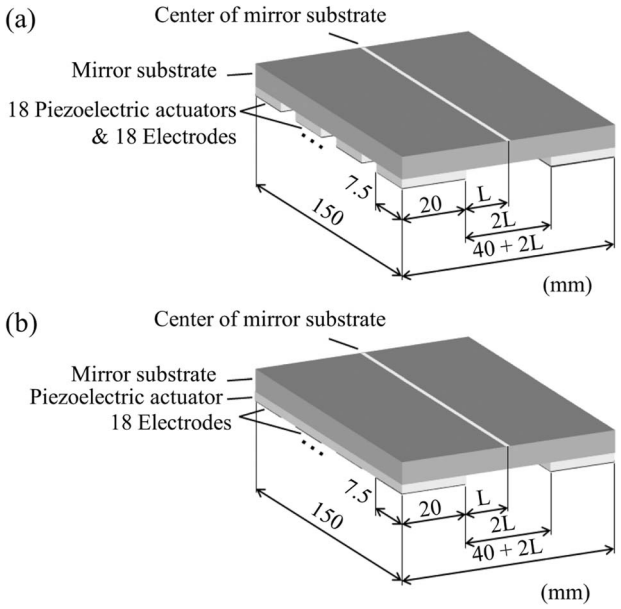

FIG. 8. (a) Separated-piezo and (b) integrated-piezo deformable mirrors modeled in FEM analysis. Other parameters are the same as those mentioned above.

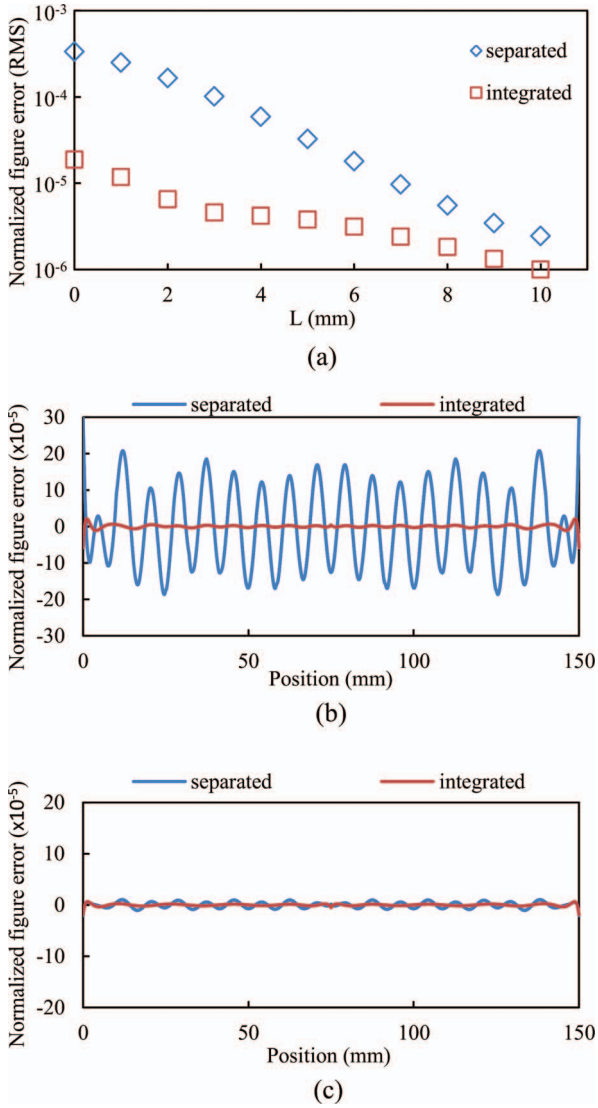

FIG. 9. (a) Relationship between distance from edge of piezoelectric actuators (L) and root mean square (RMS) HSF deformation error normalized by the maximum deformation depth in separated- and integrated-piezo mirrors. Obtained HSF deformation errors at (b) L = 3 and (c) 8 mm normalized by maximum deformation depth.

larger than those of the integrated-piezo mirrors and that the errors on the line on the back side of the piezoelectric actuators are approximately 10 times larger than those at the center.

Figures 6 and 7 show the reflection images obtained. For the separated-piezo mirror, a stripe pattern was observed for both the line on the back side of the piezoelectric actuators and the center line. The amplitude of the pattern from the line on the back side of the actuators was approximately 10 times larger than that of the line at the center. For the integrated-piezo mirror, a faint stripe pattern from the line on the back side of the piezoelectric actuators was observed. However, no pattern was observed from the line at the center. These results are consistent with those of the shape measurements and the FEM analysis.

All the obtained data show that the HSF deformation errors were caused by gaps between the electrodes. The FEM analysis revealed that separated-piezoelectric mirrors are more sensitive to deformation errors than integrated piezoelectric mirrors due to the significant stress concentration at the edge of the piezoelectric actuators. The deformation errors on the mirror surface decreased with increasing distance from the piezoelectric actuators because the uneven stress distribution on the surface due to the stress concentrations at the edge of the actuators decreased with increasing distance (see Figs. 8–10). Figure 8 shows the model deformable mirrors used in the FEM analysis. Figure 9 shows the relationships calculated by FEM between the height of the HSF deformation errors and the distance from the edge of the piezoelectric actuators along the direction from the piezoelectric actuator to the center of the substrate. The errors were normalized by the maximum deformation depth due to differences in the deformation amplitudes. Figure 10 shows the calculated principal stress distributions of the modeled mirrors. We found that distances of at least 3 and 8 mm should be used for integrated and separated piezoelectric mirrors, respectively, to sufficiently reduce the errors in our design.

For the separated piezoelectric mirror, 2 nm PV bumps formed on the processed surface on the line on the back side of the actuators. The deformable mirrors are very sensitive to changes in temperature due to the monomorph structure that the piezoelectric actuators are adhered to on the back of the substrate. During our shape measurements, the temperature appeared to change by 0.1 °C. The mirror deformation produced by this temperature change is approximately the same as that when the same voltage is applied to all the electrodes. The temperature change produced the same HSF deformation errors as those produced by the applied voltage. This indicates that the largest bumps remained on the line on the back side of the actuators in the separated piezoelectric mirror after figure correction.

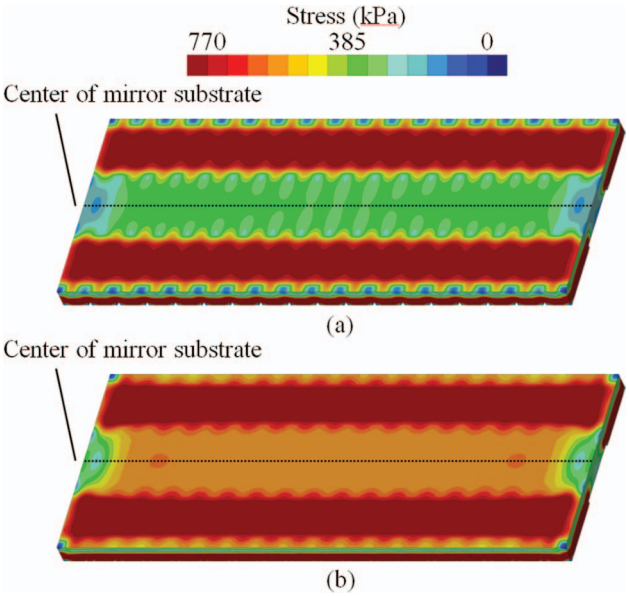

FIG. 10. Calculated distributions of principal stress on the face of (a) separated-piezo and (b) integrated-piezo mirrors. The used parameters are the same as those shown in Fig. 8 (L = 10 mm).

V. SUMMARY

To develop deformable mirrors that do not suffer from HSF deformation errors, deformation errors were investigated in detail by FEM analysis, shape measurement, and observation of x-ray reflection images. The results obtained consistently showed that an integrated-piezo structure gives lower deformation errors than a separated-piezo structure. In addition, the errors decreased with increasing distance from the piezoelectric actuators. The findings of this study have important implications for designing deformable mirrors. The development of ultraprecise deformable mirrors will enable adaptive focusing optics to be fabricated that can change the optical parameters and perform wavefront correction. Such adaptive optics will be powerful tools for x-ray analysis and microscopy.

ACKNOWLEDGMENTS

This research was mainly supported by CREST from the Japan Science and Technology Agency (JST). It was also partially supported by the Global COE Program "Center for Excellence for Atomically Controlled Fabrication Technology" from the Ministry of Education, Culture, Sports, Science and Technology, Japan. The use of BL29XUL at SPring-8 was supported by RIKEN. We would like to acknowledge JTEC Corporation for helping to process the mirror substrates by EEM.

[1]H. Mimura, S. Handa, T. Kimura, H. Yumoto, D. Yamakawa, H. Yokoyama, S. Matsuyama, K. Inagaki, K. Yamamura, Y. Sano, K. Tamasaku, Y. Nishino, M. Yabashi, T. Ishikawa, and K. Yamauchi, Nat. Phys. **6**, 122 (2010).
[2]T. Kimura, S. Handa, H. Mimura, H. Yumoto, D. Yamakawa, S. Matsuyama, K. Inagaki, Y. Sano, K. Tamasaku, Y. Nishino, M. Yabashi, T. Ishikawa, and K. Yamauchi, Jpn. J. Appl. Phys. **48**, 072503 (2009).
[3]J. Susini, D. Labergerie, and L. Zhang, Rev. Sci. Instrum. **66**, 2229 (1995).
[4]R. Signorato, O. Hignette, and J. Goulon, J. Synchrotron Radiat. **5**, 797 (1998).
[5]R. Signorato and T. Ishikawa, Nucl. Instrum. Methods **468**, 271 (2001).
[6]K. J. S. Sawhney, S. G. Alcock, and R. Signorato, Proc. SPIE **7803**, 780303 (2010).
[7]J. P. Sutter, S. G. Alcock, and K. J. S. Sawhney, Proc. SPIE **8139**, 813906 (2011).
[8]K. Yamauchi, H. Mimura, K. Inagaki, and Y. Mori, Rev. Sci. Instrum. **73**, 4028 (2002).
[9]K. Yamauchi, K. Yamamura, H. Mimura, Y. Sano, A. Saito, K. Ueno, K. Endo, A. Souvorov, M. Yabashi, K. Tamasaku, T. Ishikawa, and Y. Mori, Rev. Sci. Instrum. **74**, 2894 (2003).
[10]A. Souvorov, M. Yabashi, K. Tamasaku, T. Ishikawa, Y. Mori, K. Yamauchi, K. Yamamura, and A. Saito, J. Synchrotron Radiat. **9**, 223 (2002).
[11]H. Mimura, K. Yamauchi, K. Yamamura, A. Kubota, S. Matsuyama, Y. Sano, K. Ueno, K. Endo, Y. Nishino, K. Tamasaku, M. Yabashi, T. Ishikawa, and Y. Mori, J. Synchrotron Radiat. **11**, 343 (2004).
[12]K. Yamauchi, K. Yamamura, H. Mimura, Y. Sano, A. Saito, K. Ueno, A. Souvorov, K. Tamasaku, M. Yabashi, T. Ishikawa, and Y. Mori, Appl. Opt. **44**, 6927 (2005).